PAPER • OPEN ACCESS

Determination of uniaxial tensile strength of brittle materials using tubular samples

View the article online for updates and enhancements.

Determination of uniaxial tensile strength of brittle materials using tubular samples

D J Guerrero-Miguel[1], M I Alvarez-Fernández[1], M B Prendes-Gero[2] and C González-Nicieza[1]

[1] Department of Exploitation and Prospecting of Mines, University of Oviedo, Asturias, Spain
[2] Department of Construction and Manufacturing Engineering, University of Oviedo, Asturias, Spain

Inma@dinrock-uniovi.com

Abstract. Tensile strength of brittle materials is usually obtained through Brazilian tests. It is accepted that failure is initiated at the centre of the sample and that it propagates through the material, creating a tensile failure plane along the vertical diameter or at the majority of it. Then, the tensile stress developed at the centre of the disc is considered as the tensile strength of the material tested. However, the stress state along the vertical diameter is always biaxial, even in the centre of the sample. This implies that the strength measured using such technique is not the uniaxial tensile strength. In this article, the expressions of the stress state supported by a tubular sample subjected to a novel device to determine the tensile strength of brittle materials are described. Besides, it is noticed that the failure plane contains points with the maximum uniaxial tensile strengths so the testing method is adequate to determine the uniaxial tensile strength of brittle materials.

1. Introduction

Two of the problems in the calculation of the tensile strength of brittle materials with the universal tensile machine are: the very often breakage of the sample when it is fixed to the jaws of the machine and, the development of micro cracks inside the sample that, although imperceptible to the eyes, produce a deviation in the final value of the tensile strength.

The Brazilian test avoids these problems since it does not need to fix the sample to the jaws because the material is engaged to the jaw at the same time that a stress state is induced in the sample. In addition, in this type of material, obtaining samples with cylindrical geometry is easy. Besides, it is possible to obtain other mechanical properties of the material such as Young's modulus or Poisson's ratio [1 - 3].

However, the results from the Brazilian test are valid when the breakage starts in the centre of the sample, that is to say, the breakage happens along the vertical diameter avoiding the appearance of wedges in the vicinity of the contact. In other case, it would be necessary to determine the exact point of the breakage, analyse the stress state in the point, and look for a point along the vertical diameter that presents uniaxial stress state [4]. But the biaxiality of the Brazilian test prevents obtaining the real value of the uniaxial tensile strength of the material, obtaining values lower than real one.

This could be considered advantageous from a strength point of view, but it is a drawback to break brittle materials by excavation process. It produces an increase in the dimensioning of the machines and

mining extraction tools, as well as of all those mechanical systems used in civil engineering to break the rock mass. This poor sizing can cause the failure and even breakage of those elements and generate financial overheads or unwanted temporary delays.

In this paper a new system for characterizing brittle materials is developed. It avoids fixing the sample of the material to the testing machine. Furthermore, it makes a stress state in which the breakage of the sample begins at points exclusively subjected to tensile stress, that is, to uniaxial stress state.

The following section presents the test device developed by the Group of research DinRock of the University of Oviedo. Next, the analytical formulation for its use is developed and the results obtained in tests carried out with the novel device are analysed. The results allow to affirm that the device is suitable for determining the tensile strength in brittle materials

2. Novel tensile device

The tensile device (figure 1) is made up of four steel pieces. Two edges (number 1 in figure 1) and two cylindrical pieces called couplers (number 2 in figure 1). Figure 2 shows a detailed perspective view of both components.

The edges are composed by two geometric bodies:

- A cylindrical base with a diameter of 52 mm and a height of 8.5 mm. Its objective is to provide stability to the device along the performance of the test.
- An isosceles trapezoidal prism that transforms the displacement of the wedge along Z axis into displacement in the couplers along Y axis and whose dimensions are: 32 mm of greater base, 12 mm of smaller base and an angle of 18 ° between the Z axis and its non-parallel sides.

The couplers are formed by the juxtaposition of two cylinders of 55 and 32 mm in diameter and lengths of 3.5 and 59 mm respectively. They are cut along their longitudinal mid-plane where a groove with a thick of 8.4 mm and an inclination of 50º is machined.
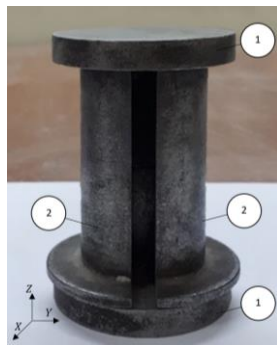

| Figure 1. Tensile device. | Figure 2. Elements of the device. |

The samples have tubular geometry (figure 3) and the tensile device is introduced inside the sample producing tensile stress without fixing the sample to jaws (figure 4). Furthermore, the contact between the outer border of the couplers and the inner border of the sample is considered to be perfect and uniform throughout all the generatrices. This contact allows to reduce the elastic problem of a three-dimensional solid to a two-dimensional one and transform the analysis from a tube to a circular ring under the hypothesis of plane elasticity.

The device-sample assembly is placed in the vertical press with its Z axis in the axis of the press (figure 4). In such a way that, as the press descends, the wedges advance over the groove of the couplers. The difference in inclination between the wedge and the groove produces that the coupler moves in a perpendicular direction to the sense of the movement and increases the load applied at the inner border of the sample. Taking into account the interaction of the components of the device and that this one is more rigid than the materials of the sample, the maximum displacement of the sample on the Y direction must be located, a priori, on the Y axis. Besides, for reasons of symmetry, the tangential displacements must be zero in both X and Y axes.

Figure 3. Sample with tubular geometry.

Figure 4. Tensile device plus sample.

A schematic representation of the transversal section of the tensile device as its mid-height with all its elements in perfect contact and the sample implemented is shown in figure 5, where the couplers are represented in orange, the wedges in green and the sample in white colour. X and Y axes have been interrupted on figure 5 at their intersections with the outer boundary to ease its graphical interpretation.
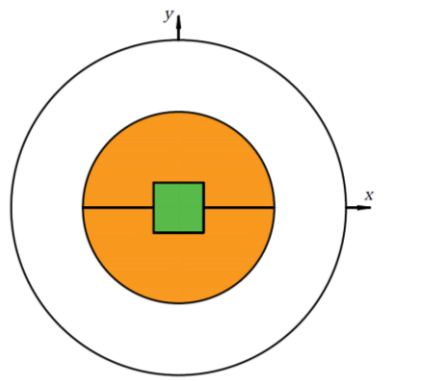

Figure 5. Sample with tubular geometry.

3. Mathematical development

Considering that the load transmitted from the device to the sample is uniformly distributed along the same generatrix, the problem is reduced to the application of plane elasticity in a circular ring [5] with inner radius R_{in} and outer radius R_{out}. The outer radius is also referred as R to simplify the notation. Henceforth, r defines the radial distance of the point considered and θ defines the angle subtended by its radius and the X axis, as shown on figure 6. Points that are initially in contact between the testing device and the sample remain in contact along the test due to the higher stiffness of the first one. Consequently, as the maximum displacement in Y direction occurs on the Y axis and the smallest on the X axis for symmetry reasons, a stress distribution is imposed with a maximum in the Y axis and zero in the X axis. Therefore, the modulus of the stress distribution varies according to the law $p\sin\theta$ and its direction is collinear to the Y axis. Note that the outer border of the sample is fully discharged. These assumptions made on the stress distribution are reasonable as long as the stiffness of the testing device remains significantly higher than the one of the sample. In other case, a more detailed analyses of the distribution imposed along the inner boundary should be done. The value of p is obtained considering that the total horizontal load (P_h) applied to the sample on the Y direction satisfies the equation (1), where α is the ratio between the inner radius (R_{in}) and the outer radius of the sample (R_{out}) and L is the total length, or height, of the sample.

$$P_h = \int_0^\pi \alpha RLp \sin\theta \, d\theta = 2\alpha RLp \tag{1}$$

Considering the equilibrium of forces on the wedge, it is possible to obtain the relation between the total horizontal load (P_h) and the total vertical load (P_v), applied along Z direction as shown in equation (2). In it, β is the angle of the wedge and μ the coefficient of friction between the wedges and the couplers.

$$P_h = \frac{P_v(-\mu \sin\beta + \cos\beta)}{2(\sin\beta + \mu\cos\beta)} \tag{2}$$

It could be considered that total applied load is $2P_h$. However, as the proposed formulation has been developed to a straightforward implementation in mechanics materials laboratories, the variable P_h relates to the total applied load recorded by the loading device in a similar form to the Brazilian test, where the total applied load is usually denoted by P. If the components of the tensional vector on the inner boundary are called T_x and T_y respectively, the tensional vector can be expressed as:

$$T_x + iT_y = ip\sin\theta \tag{3}$$

With the end of determining the stress state inside the elastic solid, techniques of complex variables have been employed. The components of stress can then be written as a function of two potentials $\phi(z)$ and $\psi(z)$:

$$\sigma_r + \sigma_\theta = 4Re[\varphi'(z)] \tag{4}$$

$$\sigma_\theta - \sigma_r + 2i\tau_{r\theta} = 2e^{2i\theta}[\bar{z}\varphi''(z) + \psi'(z)] \tag{5}$$

To simplify the resolution of the problem, the domain considered is mapped to a circular ring defined in the plane ζ [6], with inner radius α and outer radius the unit (figure 6), according to the equation (6).
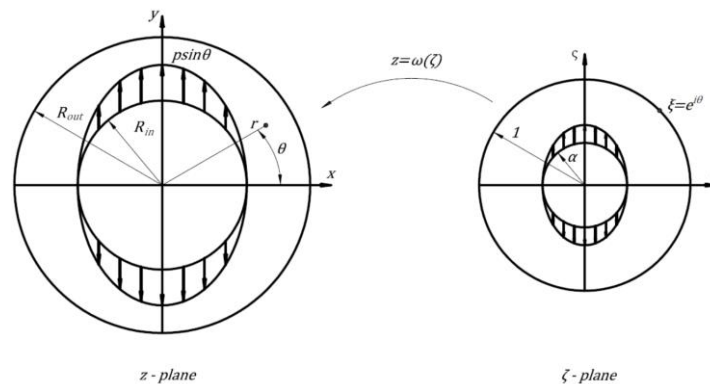
$$z = \omega(\zeta) = R\zeta \tag{6}$$

Figure 6. Graphical summary of variables for mapping from ζ plane to z plane.

By this simplification, the potentials $\phi(z)$ and $\psi(z)$ can be written in terms of the variable ζ. Furthermore, as they are analytical functions within the domain considered, they can be expressed as Laurent series:

$$\varphi(\zeta) = \sum_{k=1}^{\infty} a_k \zeta^k + \sum_{k=1}^{\infty} b_k \zeta^{-k} \tag{7}$$

$$\psi(\zeta) = c_0 + \sum_{k=1}^{\infty} c_k \zeta^k + \sum_{k=1}^{\infty} d_k \zeta^{-k} \tag{8}$$

Therefore, the boundary conditions at the outer and inner borders are given as follows [7-9]:

$$F_{out}(\xi) = \varphi(\xi) + \frac{\omega(\xi)}{\omega'(\xi)}\overline{\varphi'(\xi)} + \overline{\psi(\xi)} \tag{9}$$

$$F_{in}(\alpha\xi) + C = \varphi(\alpha\xi) + \frac{\omega(\alpha\xi)}{\omega'(\alpha\xi)}\overline{\varphi'(\alpha\xi)} + \overline{\psi(\alpha\xi)} \tag{10}$$

However, on the outer border there are no applied loads, therefore $F_{out}(\xi) = 0$, and expressing the boundary conditions on the inner border, as function of θ, $F_{in}(\alpha\xi)$ is calculated according to:

$$F_{in}(\theta) = i \int_\gamma (T_x + iT_y)ds = i \int_0^\theta -ip \sin\theta \alpha R d\theta = -p\alpha R \cos\theta \qquad (11)$$

On the other hand, the function F_{in} can be expressed as Fourier series according to equation (12), in which the term $\cos\theta$ has been rewritten in exponential form, taking to account that $\xi = \cos\theta + i\sin\theta$.

$$-\frac{p\alpha R}{2}(\xi + \xi^{-1}) = \sum_{k=-\infty}^{\infty} B_k \xi^k \qquad (12)$$

Substituting the equations (6), (7), (8) and (12) in the equations (9) and (10) it is possible to obtain the expression of the potentials $\phi(z)$ and $\psi(z)$ identifying powers of the same order [7, 8]. The expression of the components of the stress state in cylindrical coordinates are obtained from equations (4), and (5) and shown in equations (13), (14) and (15).

$$\sigma_r = -\frac{p\alpha^2(R^2-r^2)}{2r^4(\alpha^2-1)^3}\{-r^2(\alpha^2-1)^2 + \cos 2\theta [4r^2 + (\alpha^2+1)(-3R^2\alpha^2+\alpha^2 r^2)]\} \qquad (13)$$

$$\sigma_\theta = -\frac{p\alpha^2}{2R^2(\alpha^2-1)^3}\left\{\frac{3R^6\alpha^2(\alpha^2+1)\cos 2\theta + r^2 R^4(\alpha^2-1)^2}{r^4} + R^2(\alpha^2-1)^2 + \cos 2\theta (4R^2 + R^2\alpha^2 + R^2\alpha^4 - 12r^2)\right\} \qquad (14)$$

$$\tau_{r\theta} = \frac{p\alpha^2(R^2-r^2)\sin 2\theta}{2R^2 r^4(\alpha^2-1)^3}[R^2\alpha^2(\alpha^2+1)(3R^2+r^2) - 2R^2 r^2 - 6r^4] \qquad (15)$$

4. Results of the tests with the novel device

The stress and strain states are analysed employing different samples. Along the tests, the applied total load, the length of the sample and the inner radius of it are kept constant. The analysis of the influence of the thickness of the sample in the results is carried out using values of α equal to 0.2 and 0.4. In order to facilitate the interpretation of the results, the figures are modified by keeping the outer radius constant and varying the inner radius, and the comparison of the results is carried out after normalizing the values. Tensile stresses are considered positive whereas compression ones are considered negative.

4.1. Stress state

4.1.1. Normalised radial component of stress $\sigma_r/\sigma_{\theta max}$. The stress imposed by the couplers on the inner border of the sample tries to separate the sample into two halves. Therefore, tensile stress appears in the X axis and compressive stress in the Y axis (figure 7). Furthermore, the radial stress is cancelled along the outer border and at the points $z = \pm \alpha R$. On the other hand, an increase in the value of α produces an increase in the area with stress close to the maximum and an increase in the normalized distance with respect to the inner border at which the maximum or minimum stress happens.
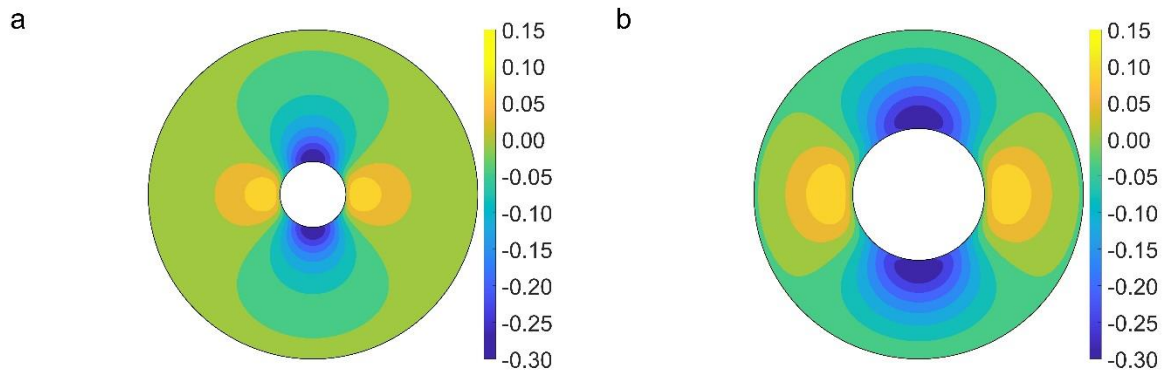
Figure 7. Normalised radial component of stress. Values of α=0.2 (a) and α=0.4 (b).

4.1.2. Normalised tangential component of stress $\sigma_\theta/\sigma_{\theta max}$. Separating the sample into two symmetrical halves implies that in the *X* axis the tangential stress reaches the highest tensile values (figure 8) and in the *Y* axis the highest compressive values. In addition, both tensile and compressive values are in the points near the border of the sample. This is because the external fibers tend to stretch due to the stress produced inside the sample. The maximum tangential stress happens at points on the inner border of the sample, and they vary with the thickness of the sample in such a way that a decrease in thickness produces a greater normalized tangential stress.
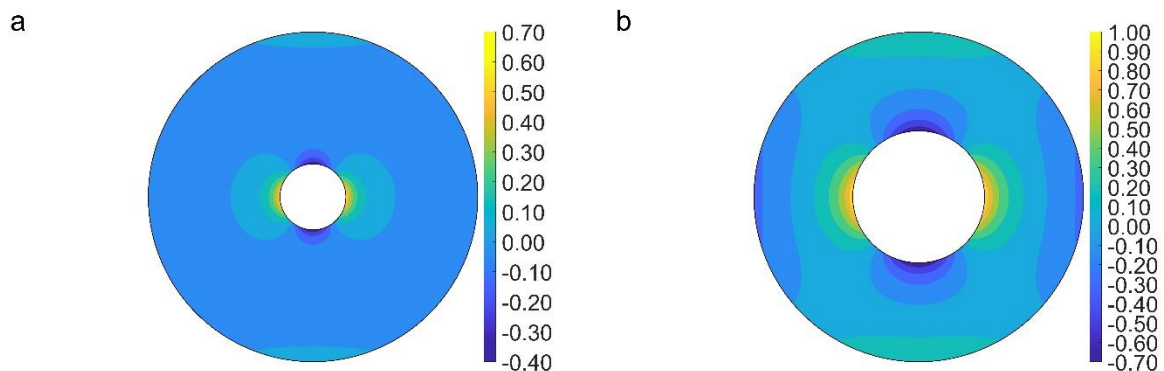

Figure 8. Normalised tangential component of stress. Values of α=0.2 (a) and α=0.4 (b).

4.1.3. Normalised shear component of stress $\tau_{r\theta}/\sigma_{\theta max}$. Due to the symmetry in the load distribution imposed on the inner border, both *X* and *Y* axes are main directions and therefore there are no shear stress in them. In any other diameter, and when advancing on the same radius, the stress changes its sign to get the value zero in the outer border (figure 9). The absolute value of the tension is equal in the four quadrants although its sign changes being positive in the first and third quadrant and negative in the second and fourth quadrant.
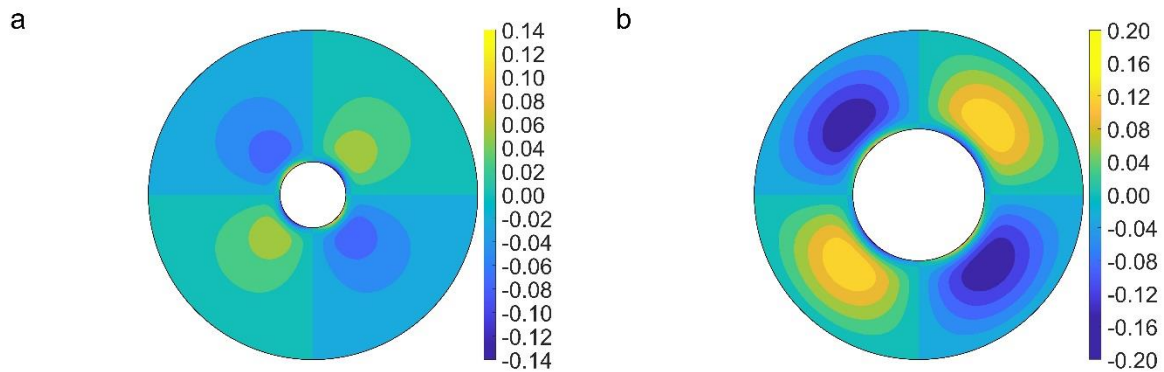
Figure 9. Normalised shear component of stress. Values of α=0.2 (a) and α=0.4 (b).

4.2. Strain state

The strain state of a sample depends on the external stress applied on it and on the mechanical properties of the material that defines the sample. For this reason, the strain state has been determined, considering conditions of plane stress on a slate sample. Table 1 shows the mechanical properties of the slate.

Table 1. Slate mechanical properties [4].

	Definition	Slate
E **(GPa)**	Young's modulus	47.55
ν	Poisson's ratio	0.24
G **(GPa)**	Transverse modulus of elasticity	19.17

4.2.1. Normalised radial component of strain $\varepsilon_r/\varepsilon_{\theta max}$. The minimum value of the radial strain is always in the intersection point between the inner border and *X* axis, while the maximum moves towards the outer border as the stiffness of the material increases (figure 10).
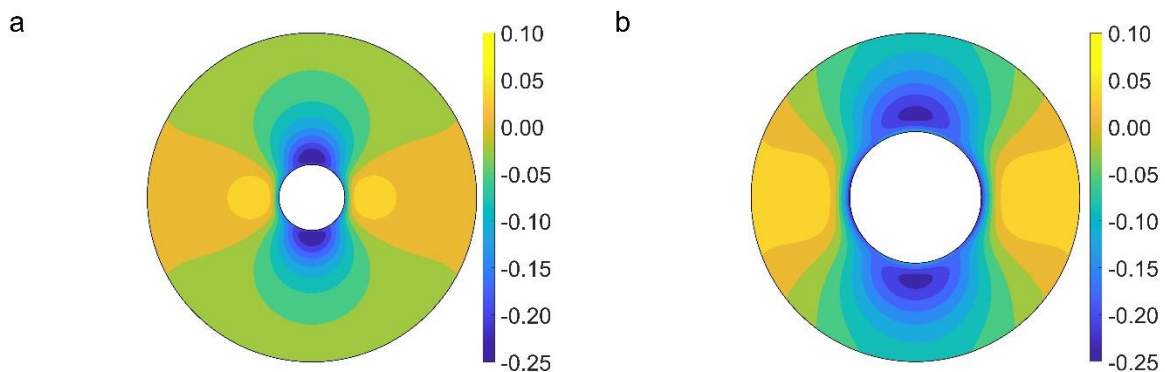

Figure 10. Normalised radial component of strain in slate. Values of α=0.2 (a) and α=0.4 (b).

4.2.2. Normalised tangential component of strain $\varepsilon_\theta/\varepsilon_{\theta max}$. The tangential strains present negative values at those points simultaneously close to the *X* axis and the outer border of the sample, with higher values in less rigid materials. However, when the value of α increases from 0.2 to 0.4 (figure 11), the tangential strains can be considered qualitatively equivalent for the different materials analysed.
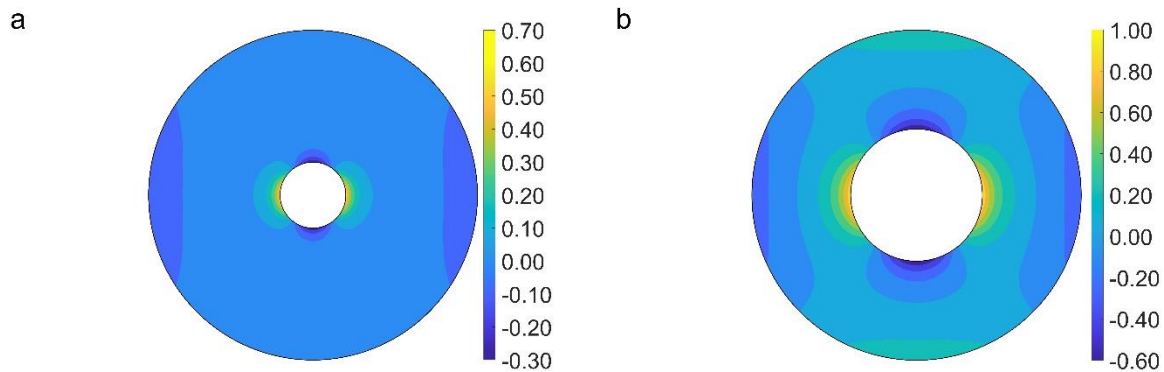
a
b

Figure 11. Normalised tangential component of strain in slate. Values of α=0.2 (a) and α=0.4 (b).

4.2.3. Normalised shear component of strain $\gamma_{r\theta}/\varepsilon_{\theta max}$. The shear strains, due to the symmetry of the stress distribution imposed, are null in both *X* and *Y* axes. Qualitatively they are equivalent for different materials, but for one sample and different values of α, the shear strains present significant variations (figure 12).
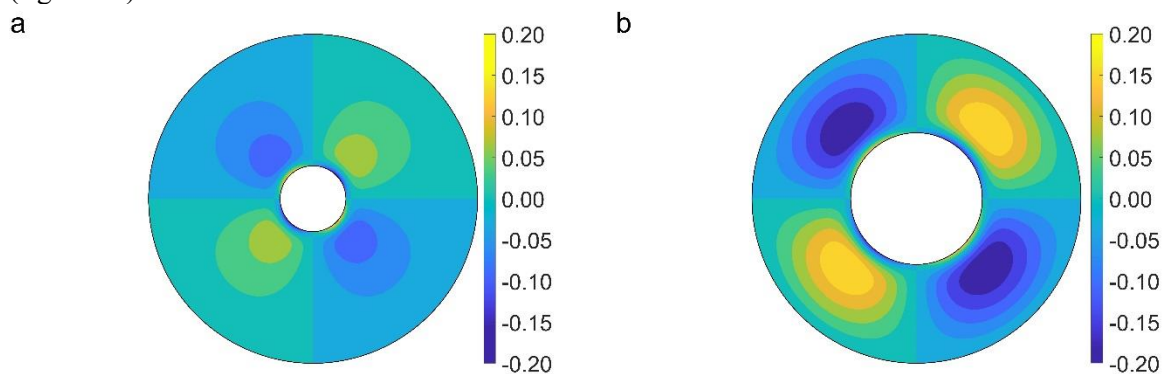
a
b

Figure 12. Normalised shear strain in slate. Values of α=0.2 (a) and α=0.4 (b).

5. Conclusions
From the results it is possible to say that:
- The implementation of the tensile device in any materials mechanics laboratory is straightforward. For its use, it is only necessary a load cell, a displacement sensor and, depending on the desired test arrangement, strain gauges.
- The stress state generated inside the sample, employing the tensile device, is similar to a composed tensile, where the *X* axis presents, at the same time, normal stress and bending moment.
- The tensile device allows to test samples under plane stress and plane strain conditions and the uniaxial tensile strength of the material without clamping the sample to the jaws of the traditional uniaxial tensile test.

References
[1]   Hondros G 1959 *The evaluation of Poisson´s ratio and the modulus of materials of a low tensile resistance by the Brazilian (indirect tensile) test with particular reference to concrete. Aust. J. Appl. Sci.* **10** 243–268

[2]   Han Y, Lai B, Liu H H, Li H 2018 *Measurement of elastic properties in Brazilian disc test: solution derivation and numerical verification. Geomech. Geophys. Geo-Energy Geo-Resources.* **4** 63–77. https://doi.org/10.1007/s40948-017-0075-1

[3]   Sgambitterra E, Lamuta C, Candamano S, Pagnotta L 2018 *Brazilian disk test and digital image correlation: a methodology for the mechanical characterization of brittle materials. Mater. Struct. Constr.* **51**. https://doi.org/10.1617/s11527-018-1145-8

[4]   Garcia-Fernandez C C, Gonzalez-Nicieza C, Alvarez-Fernandez M I, Gutierrez-Moizant R A 2018 *Analytical and experimental study of failure onset during a Brazilian test. Int. J. Rock Mech. Min. Sci.* **103** 254–265. https://doi.org/10.1016/j.ijrmms.2018.01.045

[5]   Sadd M H 2009 *Elasticity* (Oxford: Elsevier)

[6]   Ward Brown J and Churchill R V 2009 *Complex variables and applications* (New York: Mc-Graw Hill)

[7]   Sokolnikoff I S 1956 *Mathematical theory of elasticity* (New York: Mc-Graw Hill Book Company)

[8]   Muskhelishvili N I 1953 *Some basic problems of the mathematical theory of elasticity* (Tbilisi: Springer Netherlands)

[9]   Verrujit A 1996 *Complex variable solutions of elastic tunneling problems* (TU Delft: Faculteit der Civiele Techniek)